J|A|C|S ARTICLES

Published on Web 06/25/2009

Coordination Assemblies of [Mn_4] Single-Molecule Magnets Linked by Photochromic Ligands: Photochemical Control of the Magnetic Properties

Masakazu Morimoto,[†,‡] Hitoshi Miyasaka,*[,†] Masahiro Yamashita,[†] and Masahiro Irie[§]

Department of Chemistry, Graduate School of Science, Tohoku University, 6-3 Aramaki-Aza-Aoba, Aoba-ku, Sendai 980-8578, Japan, and Department of Chemistry and Research Center for Smart Molecules, Rikkyo University, 3-34-1 Nishi-Ikebukuro, Toshima-ku, Tokyo 171-8501, Japan

Received April 27, 2009; E-mail: miyasaka@agnus.chem.tohoku.ac.jp

Abstract: To achieve reversible photoswitching of the magnetic properties of single-molecule magnets (SMMs), coordination assemblies of a mixed valence tetranuclear [$Mn^{II}_2Mn^{III}_2$] complex linked by open- and closed-ring isomers of a photochromic diarylethene ligand were synthesized: [Mn_4(hmp)$_6$(dae-o)$_2$(ClO_4)$_2$]·6H_2O (open-ring form; **1o**) and [Mn_4(hmp)$_6$(dae-c)$_2$(H_2O)$_2$](ClO_4)$_2$·CH_3CN·4H_2O (closed-ring form; **1c**), where Hhmp is 2-hydroxymethylpyridine, and H_2dae-o and H_2dae-c are open- and closed-ring isomers of 1,2-bis(5-caxboxyl-2-methyl-3-thienyl)perfluorocyclopentene (H_2dae), respectively. From X-ray crystallographic analyses, **1o** and **1c** have one-dimensional (1-D) chain structures with a repeating unit of [−{Mn_4}−(dae)−], in which the [Mn_4] units are bridged by the diarylethene ligands coordinated to the Mn^{II} sites via carboxylate groups. Magnetic measurements involving direct-current (dc) and alternating-current (ac) techniques showed that each [Mn_4] cluster in the 1-D chains had an $S_T = 9$ ground state due to two kinds of intracluster ferromagnetic exchange interactions and behaved as SMMs. Both **1o** and **1c** underwent photochromic reactions in the crystalline phase, and their colors reversibly changed between reddish-brown and blue upon irradiation with ultraviolet (UV) and visible light. For **1o**, no significant change in the magnetic properties was observed after the photocyclization of the dae-o moiety by UV irradiation. In contrast, the photocycloreversion of the dae-c moiety by visible irradiation enhanced inter-[Mn_4] unit interactions in **1c**, which was triggered by the geometrical change in the diarylethene moiety during the photoreaction and the subsequent change in the inter-[Mn_4] arrangement between the neighboring 1-D chains. This work illustrates the usefulness of photochromic molecules for photoswitching the magnetic behavior of complexes, even superparamagnetic systems, with SMM units.

Introduction

Single-molecule magnets (SMMs), which display slow relaxation of the magnetization and therefore behave as nanosized magnets below blocking temperatures (T_B), have attracted much attention in a wide area of science including chemistry and physics.[1−5] The relaxation dynamics of the magnetization has been attributed to the intrinsic properties of a molecule, such as a large easy-axis-type magnetoanisotropy (negative zero-field splitting parameter: $D < 0$) and a large spin ground state (S_T), resulting in an energy barrier (Δ) of $|D|S_T^2$ for integer spins and $|D|(S_T^2 - {}^1/_4)$ for half-integer spins between spin-up and spin-down configurations, $m_s = \pm S_T$.[2] Extensive research has been performed to prepare new SMMs and to understand their magnetic properties from the viewpoints of fundamental science, such as the possibility of bridging classical and quantum regimes, and potential applications in new devices, such as single-molecule magnetic memory devices as bits due to their nanometer-scale uniform sizes[3] and quantum computers due to quantum tunneling of the magnetization (QTM).[4]

As the next step in this research field, the design of SMMs of which the magnetic properties can be reversibly switched by applying external stimuli is important and would bring about new applications for SMMs.[6] Light should be a powerful tool for switching systems because the switching behavior can be

† Tohoku University.
‡ Current address: Rikkyo University.
§ Rikkyo University.

(1) (a) Boyd, P. D. W.; Li, Q.; Vincent, J. B.; Folting, K.; Chang, H.-R.; Streib, W. E.; Huffman, J. C.; Christou, G.; Hendrickson, D. N. *J. Am. Chem. Soc.* **1988**, *110*, 8537. (b) Caneschi, A.; Gatteschi, D.; Sessoli, R. *J. Am. Chem. Soc.* **1991**, *113*, 5873. (c) Sessoli, R.; Tsai, H.-L.; Schake, A. R.; Wang, S.; Vincent, J. B.; Folting, K.; Gatteschi, D.; Christou, G.; Hendrickson, D. N. *J. Am. Chem. Soc.* **1993**, *115*, 1804.
(2) (a) Christou, G.; Gatteschi, D.; Hendrickson, D. N.; Sessoli, R. *MRS Bull.* **2000**, *25* (11), 66. (b) Gatteschi, D.; Sessoli, R. *Angew. Chem., Int. Ed.* **2003**, *42*, 268.
(3) Dahlberg, E. D.; Zhu, J.-G. *Phys. Today* **1995**, *48* (4), 34.
(4) (a) Friedman, J. R.; Sarachik, M. P.; Tejada, J.; Maciejewski, J.; Ziolo, R. *J. Appl. Phys.* **1996**, *79*, 6031. (b) Thomas, L.; Lionti, F.; Ballou, R.; Gatteschi, D.; Sessoli, R.; Barbara, B. *Nature* **1996**, *383*, 145. (c) Friedman, J. R.; Sarachik, M. P.; Tejada, J.; Ziolo, R. *Phys. Rev. Lett.* **1996**, *76*, 3830. (d) Hernández, J. M.; Zhang, X. X.; Luis, F.; Bartolomé, J.; Tejada, J.; Ziolo, R. *Europhys. Lett.* **1996**, *35*, 301. (e) Friedman, J. R.; Sarachik, M. P.; Hernández, J. M.; Zhang, X. X.; Tejada, J.; Molins, E.; Ziolo, R. *J. Appl. Phys.* **1997**, *81*, 3978. (f) Leuenberger, M. N.; Loss, D. *Nature* **2001**, *410*, 789.

Scheme 1[a]

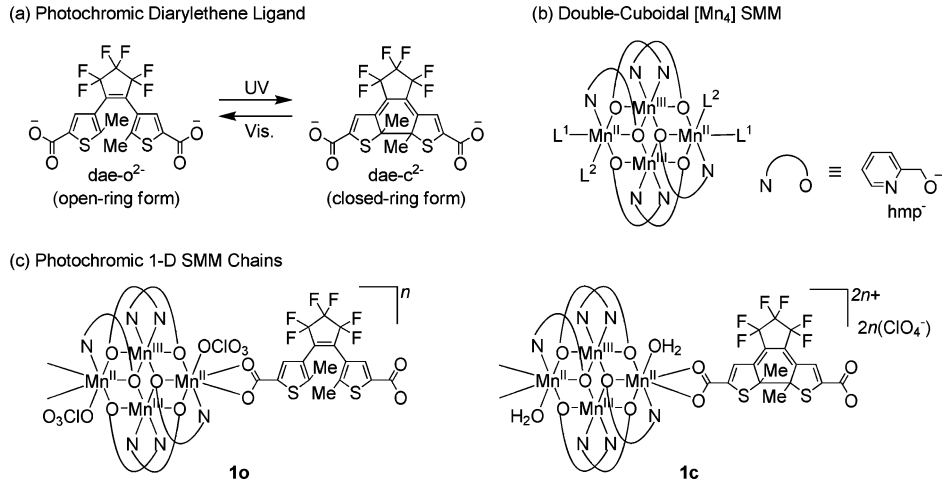

[a] (a) Photochromic diarylethene ligand with two carboxylate groups (dae-o^{2-}: open-ring isomer, dae-c^{2-}: closed-ring isomer), (b) double-cuboidal [Mn_4] single-molecule magnet, and (c) 1-D coordination assemblies of [Mn_4] single-molecule magnets linked by the photochromic diarylethene ligands in the open- and closed-ring forms, **1o** and **1c**.

controlled precisely in a wide range of the resolutions of time and space. Herein, we present a reversible photoswitching system involving 1-D chain coordination assemblies comprised of SMMs and photochromic molecules (Scheme 1). The photochromic molecules not only undergo a reversible color change but also change other chemical and physical properties upon photoisomerization.[7] Various photochromic compounds have been synthesized and investigated for application in molecular memory and switching devices.[8] We chose a photochromic diarylethene ligand, dae^{2-}, which had two carboxylate groups at 5-positions on thiophene rings as shown in Scheme 1a (dae^{2-} stands for the deprotonated dianion of 1,2-bis(5-caxboxyl-2-methyl-3-thienyl)perfluorocyclopentene (H_2dae),[9] and dae-o^{2-} and dae-c^{2-} are open and closed-ring isomers, respectively) to act as a photoswitch and cluster linkages. dae^{2-} reversibly isomerizes between open- and closed-ring isomers when irradiated with UV and visible light via 6π electrocyclic reactions of the 1,3,5-hexatriene moieties in the molecules.[10] A remarkable feature of the diarylethene derivatives is that they show thermally stable and fatigue-resistant photochromic performance not only in solution but also in the single-crystalline phase.[11] Several examples involving the photoswitching of single-molecule fluorescence and conductivity via the photochromic reaction of diarylethene ligand have been reported.[12] Using the diarylethene groups to bridge the SMMs should bring about the following for the photoreversible modulation of magnetic properties: (I) direct switching of superexchange interactions through the π-system of the diarylethene (Scheme 2a) and (II) indirect switching of through-space interactions between SMM units due to structural changes (Scheme 2b). In the case of direct switching, the structure of the π-system of the open- and closed-ring isomers is different. The π-conjugation of the two thiophene rings are separated in the open-ring isomer, whereas it is expanded over the entire molecule in the closed-ring isomer.[10] Therefore, the photoreversible change in π-conjugation of the diarylethene moiety should cause a change in the superexchange interactions between the combined SMM units (intrachain switching; Scheme 2a), resulting in dynamic photoswitching behavior via an "exchange-bias" effect on the magnetization relaxation of the SMM unit.[13] As a representative example for this case, photoswitching of the magnetic interactions between two nitronyl nitroxide radicals bridged by diarylethene molecules has been reported.[14] Indirect switching should occur when the geometrical structures reversibly change upon photochromic reaction, as X-ray crystallographic studies have shown.[11a,b] This change should cause the packing of the

(5) (a) Wernsdorfer, W.; Sessoli, R. *Science* **1999**, *284*, 133. (b) Wernsdorfer, W.; Sessoli, R.; Caneschi, A.; Gatteschi, D.; Cornia, A.; Mailly, D. *J. Appl. Phys.* **2000**, *87*, 5481. (c) Wernsdorfer, W.; Soler, M.; Christou, G.; Hendrickson, D. N. *J. Appl. Phys.* **2002**, *91*, 7164. (d) Wernsdorfer, W.; Chakov, N. E.; Christou, G. *Phys. Rev. Lett.* **2005**, *95*, 037203.
(6) Miyasaka, H.; Yamashita, M. *Dalton Trans.* **2007**, 399.
(7) (a) Brown, G. H. *Photochromism*; Wiley-Interscience: New York, 1971. (b) Dürr, H.; Bouas-Laurent, H. *Photochromism: Molecules and Systems*; Elsevier: Amsterdam, 2003.
(8) (a) Irie, M. *Photo-Reactive Materials for Ultrahigh-Density Optical Memories*; Elsevier: Amsterdam, 1994. (b) Feringa, B. L., Ed. *Molecular Switches*; Wiley-VCH: Weinheim, 2001.
(9) Morimoto, M.; Irie, M. *Chem.—Eur. J.* **2006**, *12*, 4275.
(10) (a) Irie, M. *Chem. Rev.* **2000**, *100*, 1685–1716. (b) Tian, H.; Yang, S. *Chem. Soc. Rev.* **2004**, *33*, 85.
(11) (a) Yamada, T.; Kobatake, S.; Muto, K.; Irie, M. *J. Am. Chem. Soc.* **2000**, *122*, 1589. (b) Yamada, T.; Kobatake, S.; Irie, M. *Bull. Chem. Soc. Jpn.* **2000**, *73*, 2179. (c) Kobatake, S.; Uchida, K.; Tsuchida, E.; Irie, M. *Chem. Commun.* **2002**, 2804. (d) Kobatake, S.; Irie, M. *Bull. Chem. Soc. Jpn.* **2004**, *77*, 195. (e) Morimoto, M.; Irie, M. *Chem. Commun.* **2005**, 3895. (f) Kobatake, S.; Takami, S.; Muto, H.; Ishikawa, T.; Irie, M. *Nature* **2007**, *446*, 778. (g) Irie, M. *Bull. Chem. Soc. Jpn.* **2008**, *8*, 917.
(12) (a) Irie, M.; Fukaminato, T.; Sasaki, T.; Tamai, N.; Kawai, T. *Nature* **2002**, *420*, 759. (b) Dulić, D.; van der Molen, S. J.; Kudernac, T.; Jonkman, H. T.; de Jong, J. J. D.; Bowden, T. N.; van Esch, J.; Feringa, B. L.; van Wees, B. J. *Phys. Rev. Lett.* **2003**, *91*, 207402. (c) Katsonis, N.; Kudernac, T.; Walko, M.; van der Molen, S. J.; van Wees, B. J.; Feringa, B. L. *Adv. Mater.* **2006**, *18*, 1397.
(13) (a) Wernsdorfer, W.; Aliaga-Alcalde, N.; Hendrickson, D. N.; Christou, G. *Nature* **2002**, *416*, 406. (b) Wernsdorfer, W.; Bhaduri, S.; Tiron, R.; Hendrickson, D. N.; Christou, G. *Phys. Rev. Lett.* **2002**, *89*, 197201. (c) Park, K.; Pederson, M. R.; Richardson, S. L.; Aliaga-Alcalde, N.; Christou, G. *Phys. Rev. B* **2003**, *68*, 020405. (d) Hill, S.; Edwards, R. S.; Aliaga-Alcalde, N.; Christou, G. *Science* **2003**, *302*, 1015. (e) Tiron, R.; Wernsdorfer, W.; Aliaga-Alcalde, N.; Christou, G. *Phys. Rev. B* **2003**, *68*, 140407. (f) Tiron, R.; Wernsdorfer, W.; Foguet-Albiol, D.; Aliaga-Alcalde, N.; Christou, G. *Phys. Rev. Lett.* **2003**, *91*, 227203. (g) Yang, E.-C.; Wernsdorfer, W.; Hill, S.; Edwards, R. S.; Nakano, M.; Maccagnano, S.; Zakharov, L. N.; Rheingold, A. L.; Christou, G.; Hendrickson, D. N. *Polyhedron* **2003**, *22*, 1727.
(14) (a) Matsuda, K.; Irie, M. *J. Am. Chem. Soc.* **2000**, *122*, 7195. (b) Matsuda, K.; Irie, M. *Chem.—Eur. J.* **2001**, *7*, 3466. (c) Matsuda, K. *Bull. Chem. Soc. Jpn.* **2005**, *78*, 383. (d) Tanifuji, N.; Irie, M.; Matsuda, K. *J. Am. Chem. Soc.* **2005**, *127*, 13344.

Scheme 2. Proposed Photoswitching Mechanisms in the Photochromic 1-D SMM Chains[a]

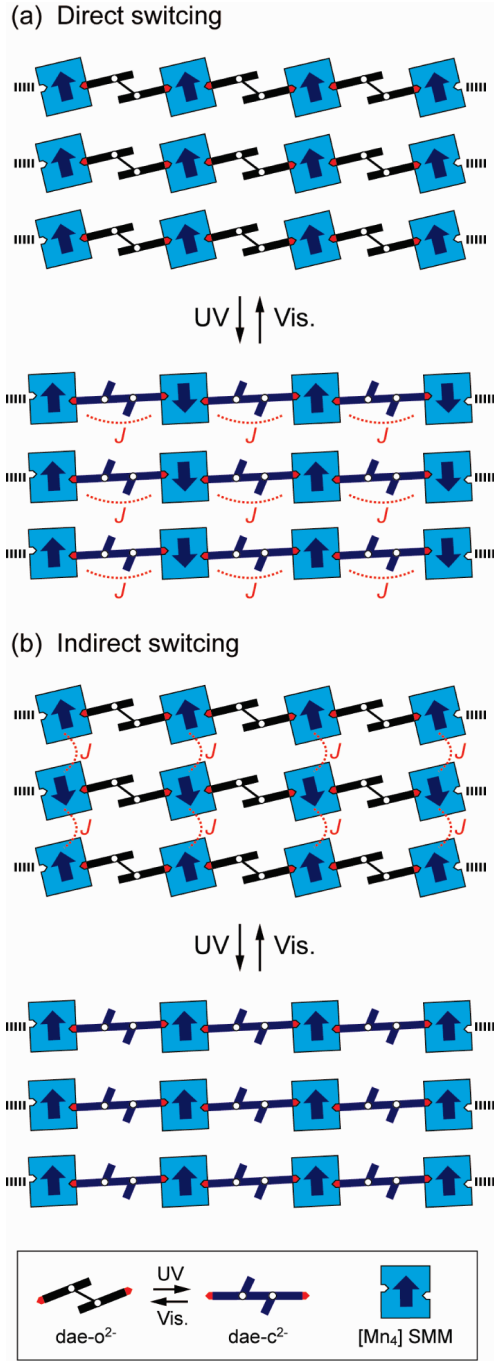

[a] (a) Direct switching of superexchange interactions due to the change in the π-system of the diarylethene ligand (intrachain switching) and (b) indirect switching of through-space interactions due to the change in the geometrical structure of the diarylethene ligand (interchain switching), where the arrows indicate the magnetization of SMM aligned on an easy axis; in the case of interacted systems of (a) and (b) with exchange couplings J, fustian antiferromagnetically coupled features were for instance illustrated.

SMM chains to change, which would indirectly lead to the modulation of the through-space magnetic interactions (interchain switching; Scheme 2b).

In this study, a double-cuboidal mixed valence [$Mn^{II}_2Mn^{III}_2$] cluster was used as the SMM unit (Scheme 1b).[15] The prototype of the SMMs [$Mn_4(hmp)_6Br_2(H_2O)_2$]$Br_2\cdot 4H_2O$ (hmp^-: deprotonated anion of 2-hydroxymethylpyridine, Hhmp), of which $S_T = 9$, has been reported.[15a] This SMM is robust and acts as a coordination-acceptor building block for SMM networks without a significant change in the core structure.[16] Using these units, we synthesized 1-D chain structures, in which the [Mn_4] units were linked by the dae^{2-} ligands in the open- and closed-ring forms: [$Mn_4(hmp)_6(dae\text{-}o)_2(ClO_4)_2]\cdot 6H_2O$ (**1o**) and [$Mn_4(hmp)_6(dae\text{-}c)_2(H_2O)_2](ClO_4)_2\cdot CH_3CN\cdot 4H_2O$ (**1c**), respectively (Scheme 1c). In this paper, we report the syntheses, crystal structures, and photochromic and magnetic properties of the 1-D SMM chains **1o** and **1c**. The effect of the photochromic reactions of the diarylethene ligand on the magnetic properties will also be discussed.

Results and Discussion

Syntheses. There are two synthetic routes for preparing assemblies of the double-cuboidal [$Mn^{II}_2Mn^{III}_2$] SMMs. One involves a one-pot reaction in which the formation of the SMM core and assembly via the bridging groups occur at the same time in a solution containing Mn sources, ligands for constructing the SMM core (hmp^-), and the bridging ligand. The other route involves the assembly of the preisolated SMM unit with the bridging ligand. At the present time, 1-D, 2-D, and 3-D assemblies of the [Mn_4] SMMs bridged by polydentate ligands, such as azide, chloride, dicyanamide, $\{Mn[N(CN)_2]_6\}^{2-}$, and $[Pt(nmt)_2]^-$ (mnt^{2-} = maleonitriledithiolate), have been synthesized using the two methods.[16] In the present study, the one-pot method was used, and the detailed procedure is described in the Experimental Section. Briefly, $Mn^{II}(ClO_4)_2$ as a Mn source was reacted with Hhmp in the presence of NEt_4OH in acetonitrile to afford the [Mn_4] core. Then, the protonated photochromic ligand H_2dae-o or H_2dae-c was added to the solution. Slow diffusion of another solvent into the resulting solution afforded black single crystals of **1o** or **1c**. Note that, during crystallization, everything must be kept in the dark, especially **1c**.

Crystal Structure of 1o. Crystallographic data for **1o** and **1c** are listed in Table 1. **1o** crystallized in the monoclinic space group $C2/c$ with a $C2$ rotation axis on the dae-o^{2-} ligand and an inversion center on the [Mn_4] unit ($Z = 4$). **1o** has an infinite 1-D chain structure, in which the [Mn_4] units are bridged by the dae-o^{2-} ligand to form an alternate arrangement [$-\{Mn_4\}-$

(15) (a) Yoo, J.; Brechin, E. K.; Yamaguchi, A.; Nakano, M.; Huffman, J. C.; Maniero, A. L.; Brunel, L.-C.; Awaga, K.; Ishimoto, H.; Christou, G.; Hendrickson, D. N. *Inorg. Chem.* **2000**, *39*, 3615. (b) Yoo, J.; Yamaguchi, A.; Nakano, M.; Krzystek, J.; Streib, W. E.; Brunel, L.-C.; Ishimoto, H.; Christou, G.; Hendrickson, D. N. *Inorg. Chem.* **2001**, *40*, 4604. (c) Hendrickson, D. N.; Christou, G.; Ishimoto, H.; Yoo, J.; Brechin, E. K.; Yamaguchi, A.; Rumberger, E. M.; Aubin, S. M. J.; Sun, Z.; Aromí, G. *Polyhedron* **2001**, *20*, 1479. (d) Yamaguchi, A.; Kusumi, N.; Ishimoto, H.; Mitamura, H.; Goto, T.; Mori, N.; Nakano, M.; Awaga, K.; Yoo, J.; Hendrickson, D. N.; Christou, G. *J. Phys. Soc. Jpn.* **2002**, *71*, 414. (e) Yang, E.-C.; Harden, N.; Wernsdorfer, W.; Zakharov, L.; Brechin, E. K.; Rheingold, A. L.; Christou, G.; Hendrickson, D. N. *Polyhedron* **2003**, *22*, 1857. (g) Lecren, L.; Li, Y.-G.; Wernsdorfer, W.; Roubeau, O.; Miyasaka, H.; Clérac, R. *Inorg. Chem. Commun.* **2005**, *8*, 626. (h) Lecren, L.; Wernsdorfer, W.; Li, Y.-G.; Roubeau, O.; Miyasaka, H.; Clérac, R. *J. Am. Chem. Soc.* **2005**, *127*, 11311.

(16) (a) Miyasaka, H.; Nakata, K.; Sugiura, K.; Yamashita, M.; Clérac, R. *Angew. Chem., Int. Ed.* **2004**, *43*, 707. (b) Lecren, L.; Roubeau, O.; Coulon, C.; Li, Y.-G.; Le Goff, X. F.; Wernsdorfer, W.; Miyasaka, H.; Clérac, R. *J. Am. Chem. Soc.* **2005**, *127*, 17353. (c) Yoo, J.; Wernsdorfer, W.; Yang, E.-C.; Nakano, M.; Rheingold, A. L.; Hendrickson, D. N. *Inorg. Chem.* **2005**, *44*, 3377. (d) Miyasaka, H.; Nakata, K.; Lecren, L.; Coulon, C.; Nakazawa, Y.; Fujisaki, T.; Sugiura, K.; Yamashita, M.; Clérac, R. *J. Am. Chem. Soc.* **2006**, *128*, 3770. (e) Hiraga, H.; Miyasaka, H.; Nakata, K.; Kajiwara, T.; Takaishi, S.; Oshima, Y.; Nojiri, H.; Yamashita, M. *Inorg. Chem.* **2007**, *46*, 9661.

Table 1. Crystallographic Data for **1o** and **1c**

	1o	**1c**
formula	$C_{53}H_{56}N_6O_{24}F_6Cl_2S_2Mn_4$	$C_{55}H_{59}N_7O_{24}F_6Cl_2S_2Mn_4$
formula weight	1629.82	1670.87
temperature/K	93	113
crystal system	monoclinic	monoclinic
space group	*C*2/*c*	$P2_1/m$
a/Å	32.50(2)	11.360(11)
b/Å	14.219(8)	27.82(2)
c/Å	14.468(9)	12.440(12)
α/deg	90	90
β/deg	104.848(6)	109.908(10)
γ/deg	90	90
V/Å^3	6464(7)	3697(6)
Z	4	2
ρ_{calcd}/g cm^{-3}	1.675	1.534
μ/cm^{-1}	10.114	8.866
F(000)	3312.00	1700.00
data measured	25 491	38 467
data unique	7287	8544
R_{int}	0.022	0.039
no. of observations (all reflections)	5650	6617
no. of variables	460	564
goodness-of-fit	1.053	1.032
R_1 ($I > 2\sigma(I)$)	0.0601	0.0959
wR_2 (all data)	0.1489	0.1983

(dae-o)−], as shown in Figure 1a (the hexafluorocyclopentene ring in dae-o^{2-} is disordered, as observed with other diarylethene derivatives (Figure S1)). An ORTEP drawing of the repeating unit in the 1-D chain structure of **1o** is shown in Figure 1b, and selected bond distances and angles in the [Mn_4] core are listed in Table S1. The [Mn_4] moiety has a typical double-cuboidal core containing two inner Mn^{III} ions (Mn(2) and Mn(2)*) and two outer Mn^{II} ions (Mn(1) and Mn(1)*),[15,16] which were assigned on the basis of bond valence sum (BVS) calculations,[17] with six hmp$^-$ bidentate ligands, forming the basic [Mn_4(hmp)$_6$]$^{4+}$ core. The core of **1c** is similar (vide infra). The inner Mn^{III} ions are hexacoordinated with an N_2O_4 atom set from the hmp$^-$ ligands, whereas the outer Mn^{II} ions are heptacoordinated with an NO_3 atom set from the hmp$^-$ ligands, two O atoms from the carboxylate groups of dae-o^{2-}, and one O atom from ClO_4^- as a capping ligand. Thus, each carboxylate group of dae-o^{2-} acts as a bidentate ligand to the outer Mn^{II} ion. The inner Mn^{III} ions Mn(2) and Mn(2)* exhibit a Jahn−Teller distortion causing them to have an elongated tetragonal geometry with the axes along O(3)*−Mn(2)−N(2)* and O(3)−Mn(2)*−N(2), respectively (Mn(2)−N(2)* = 2.127(3) Å, Mn(2)−O(3)* = 2.118(3) Å, O(3)*−Mn(2)−N(2)* = 160.86(13)°), where the two Jahn−Teller axes are parallel to each other in the [Mn_4] core because of the presence of the inversion center at the midpoint of the core.

Since the main purpose in this work involves photochromic reactions in the solid state, we should discuss here the possibility of isomerization to the closed-ring isomer from a structural point of view. The photochromic reactivity of the diarylethene derivatives in the crystalline state strongly depends on the conformation of the molecules in the crystal. To undergo the photocylization reaction, the two thiophene rings of the diarylethene moiety must be fixed in an antiparallel conformation, and the distance between the reacting carbon atoms must be less than 4 Å.[11c,18] In **1o**, the dae-o^{2-} ligand has an antiparallel conformation, and the distance between the reacting carbon atoms (C(19)···C(19)**) was determined to be 3.371 Å (Figure 1b). Thus, the requirements for the photocyclization reaction are met.

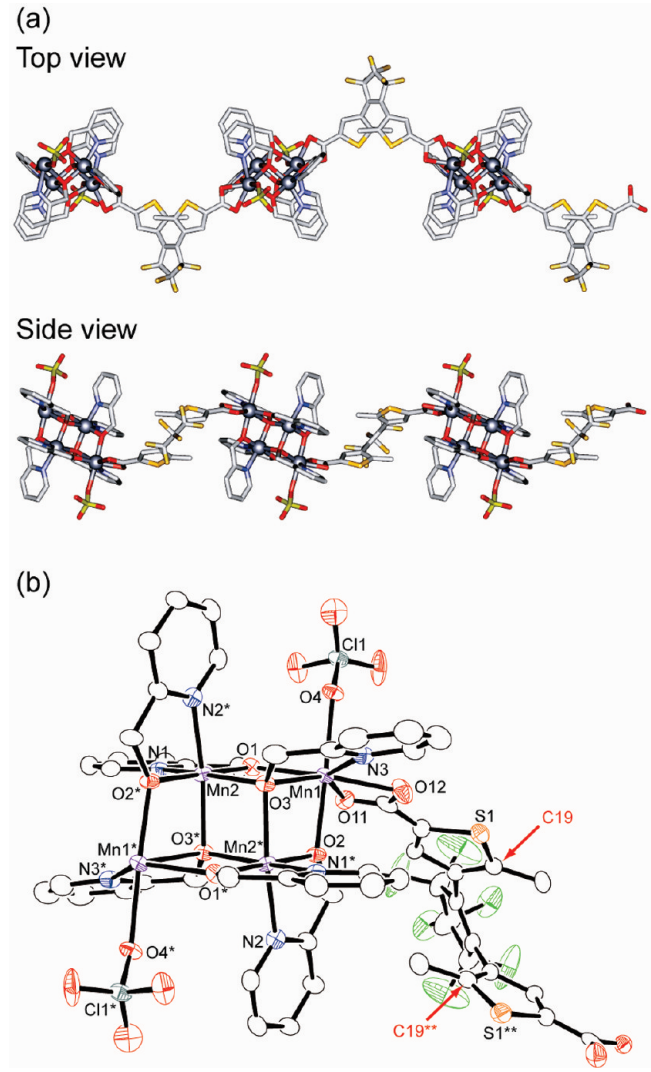

Figure 1. (a) 1-D chain structure and (b) ORTEP drawing of a repeating unit of **1o** (50% probability thermal ellipsoids). The disordered part in the dae-o^{2-} moiety and hydrogen atoms are omitted for clarity (see Figure S1). C(19) and C(19)** (indicated by red arrows) are the photoreacting carbon atoms in the dae-o^{2-} moiety. Symmetry operation (*): $-x + {}^1/_2 + 1, -y + {}^1/_2, -z + 1$; (**): $-x + 1, -y, -z + {}^1/_2$.

Figure 2 shows packing diagrams of **1o**. The 1-D chain lies in the *a*+*c* direction in the crystal lattice. The neighboring chains are in an in-phase arrangement, making alternately stacked 2-D layers of the [Mn_4] unit and the dae-o^{2-} ligand (Figure 2a). The Jahn−Teller axes in the [Mn_4] cores are also parallel to each other in the entire crystal. The interunit Mn^{II}···Mn^{II} distance in the chains across the dae-o^{2-} ligand was determined to be 12.741 Å. The nearest interchain interunit distance was found to be 8.453 Å for Mn^{II}···Mn^{III} (Figure 2b).

(17) Brown, I. D.; Altermatt, D. *Acta Crystallogr., Sect. B* **1985**, *41*, 244.
(18) The open-ring isomer of diarylethene has two conformations with the aryl rings in mirror symmetry (parallel conformation) and C_2 symmetry (antiparallel conformation). According to the Woodward−Hoffmann rule, photoinduced electrocyclic reactions of 6π systems proceed in the conrotatory mode. The conrotatory photocyclization of diarylethene can proceed only from the antiparallel conformation. See: (a) Woodward, R. B.; Hoffmann, R. *The conservation of orbital symmetry*; Verlag Chemie: Weinheim, 1970. (b) Nakamura, S.; Irie, M. *J. Org. Chem.* **1988**, *53*, 6136. (c) Uchida, K.; Nakayama, Y.; Irie, M. *Bull. Chem. Soc. Jpn.* **1990**, *63*, 1311. (d) Irie, M.; Miyatake, O.; Uchida, K. *J. Am. Chem. Soc.* **1992**, *114*, 8715.

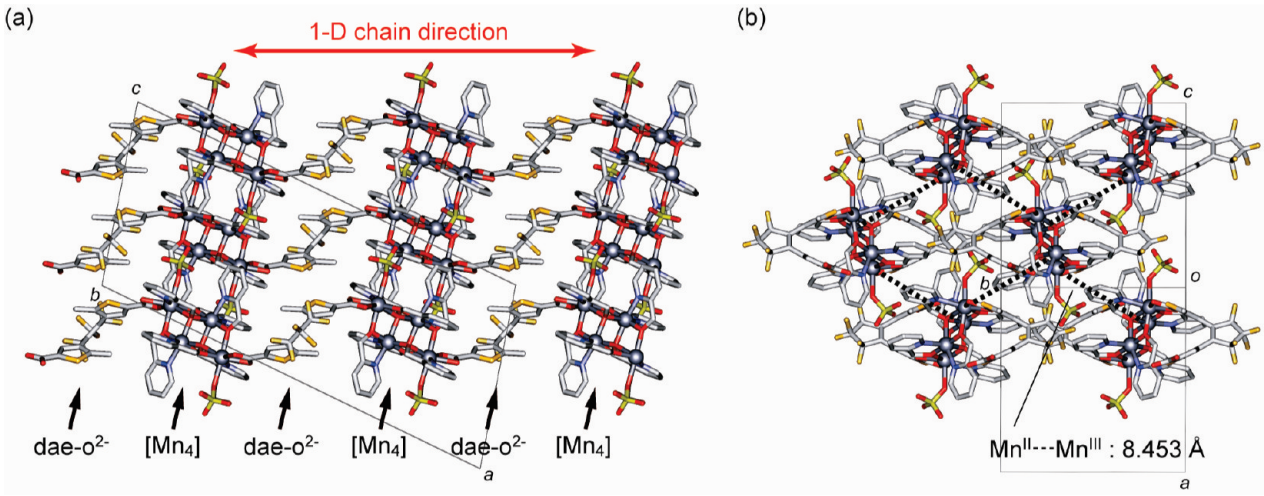

Figure 2. Packing diagrams of **1o** (a) projected along the *b* axis and (b) projected along the $a + c$ direction, i.e., parallel to the chain axis. The hydrogen atoms and the water molecules of crystallization are omitted for clarity. The dotted lines in (b) represent the closest $Mn^{II}\cdots Mn^{III}$ contacts between the $[Mn_4]$ cores in the neighboring chains.

Crystal Structure of 1c. 1c crystallized in the monoclinic space group $P2_1/m$ with an inversion center on the $[Mn_4]$ moiety and a mirror plane through the dae-c^{2-} ligand ($Z = 2$; Table 1). Similar to **1o**, **1c** has an infinite 1-D chain structure composed of $[Mn_4]$ double-cuboidal units and the dae-c^{2-} ligands in an alternating arrangement $[-\{Mn_4\}-(dae\text{-}c)-]$ (Figure 3a), in which the dae-c^{2-} ligand acts as a bidentate ligand coordinating to the outer Mn sites of the $[Mn_4]$ unit via carboxylate groups. The (*R*,*R*) and (*S*,*S*) enantiomers of dae-c^{2-} were disordered because they sit in the same site with an occupancy ratio of 1:1,[19] and the hexafluorocyclopentene ring of dae-c^{2-} was also disordered similar to that of **1o** (Figure S2). An ORTEP drawing of the repeating unit in the 1-D chain of **1c** is shown in Figure 3b, and selected bond distances and angles in the $[Mn_4]$ core are listed in Table S1. The $[Mn_4]$ moiety has a $[Mn_4(hmp)_6]^{4+}$ core. The outer and inner Mn ions were assigned to be Mn^{II} and Mn^{III} on the basis of bond valence sum (BVS) calculations[17] and structural characteristics (vide infra). As in the case of **1o**, the inner Mn^{III} ions are hexacoordinated, and the outer Mn^{II} ions are heptacoordinated. However, the terminal ligand on the Mn^{II} ion is a water molecule instead of ClO_4^- which is the terminal ligand in **1o**. The ClO_4^- ions are located between chains. The two Mn^{III} ions exhibited Jahn−Teller elongation of the O(3)*−Mn(2)−N(2)* and O(3)−Mn(2)*−N(2) axes with Mn(2)−N(2)* = 2.220(5) Å, Mn(2)−O(3)* = 2.280(3) Å, and O(3)*−Mn(2)−N(2)* = 161.19(18)°. The two Jahn−Teller axes were parallel to each other in the core. As we can see in Figure 3b, the dae-c^{2-} moiety has a closed-ring structure by making a single bond, C(19)**−C(20).

Figure 4 shows packing diagrams of **1c**. The 1-D chains are parallel to the *b* axis of the crystal lattice. The $[Mn_4]$ units and the dae-c^{2-} ligands were alternately stacked to form a 2-D layered structure (Figure 4a). The Jahn−Teller axes of the $[Mn_4]$ cores are alternately arranged in the chains with a tilt angle of about 70° because of the presence of the mirror symmetry on the dae-c^{2-} ligand. The intrachain interunit $Mn^{II}\cdots Mn^{II}$ distance across the dae-c^{2-} ligand was 13.186 Å. Different from the structure of **1o**, the interchain interunit distance (5.703 Å for $Mn^{II}\cdots Mn^{II}$) in **1c** was significantly small (Figure 4b). This close contact may give rise to magnetic interactions between the $[Mn_4]$ cores in the neighboring chains (vide infra).

DC Magnetic Measurements on 1o and 1c. Variable-temperature magnetic susceptibility measurements were carried out on microcrystalline samples of **1o** and **1c** restrained in Nujol in a 1 kOe dc field in the temperature range 1.82−300 K. The temperature dependence of χT products is shown in Figure 5. Basically, **1o** and **1c** showed similar behavior to the previously reported $[Mn_4]$ SMMs.[15,16b,d] The χT value at 300 K was ∼16 cm^3 K mol^{-1} for both compounds, which is consistent with the spin-only value expected for a set of noninteracting isotropic magnetic centers of $S_{Mn(II)} = {}^5/_2 \times 2$ and $S_{Mn(III)} = 2 \times 2$ with $g = 2$ (14.75 cm^3 K mol^{-1}), and upon lowering the temperature, it increased to a maximum of 40.65 cm^3 K mol^{-1} at 4.3 K and 36.82 cm^3 K mol^{-1} at 7.5 K for **1o** and **1c**, respectively. This increase is due to ferromagnetic interactions among the Mn ions in the $[Mn_4]$ core. Please note that the exchange couplings between the Mn^{III} ions and between the Mn^{II} and Mn^{III} ions are denoted hereafter as J_{bb} and J_{wb}, respectively. The experimental data were simulated to estimate J_{bb} and J_{wb} using the Heisenberg−Van Vleck model, which has already been used with analogous $[Mn_4]$ clusters $[\boldsymbol{H} = -2J_{bb}(\boldsymbol{S}_{Mn(III)}\boldsymbol{S}_{Mn(III)'}) - 2J_{wb}(\boldsymbol{S}_{Mn(II)} + \boldsymbol{S}_{Mn(II)'})(\boldsymbol{S}_{Mn(III)} + \boldsymbol{S}_{Mn(III)'})]$.[15a] The data below 7 K for **1o** and 13 K for **1c**, of which χT decreased, were omitted to avoid the effects of zero-field splitting (ZFS) and/or intercluster interactions. In fact, these effects were not taken into account in this simulation to avoid the overparameterization. With temperature-independent paramagnetism (TIP) fixed to 6×10^{-4} cm^3 mol^{-1}, excellent fits were obtained for both an adequate parameter set and positive values of J_{bb} and J_{wb} where $J_{bb} > J_{wb}$ (Table 2). The ranges of J_{bb} and J_{wb} are almost similar to those for related $[Mn_4]$ with $S_T = 9$.[15,16b,d]

Estimation of the Axial Zero-Field Splitting Parameter *D* on the Basis of S_T. To confirm the anisotropic nature of the spin ground state (S_T), the reduced magnetization at high fields (1−7 T) and low temperatures (1.8−4.5 K) of **1o** and **1c** was examined. Figure 6 shows plots of $M/N\mu_B$ vs H/T, where M is the magnetization, N is Avogadro's number, μ_B is the Bohr magneton, and H is the applied magnetic field. At $H = 7$ T and $T = 1.8$ K, **1o** and **1c** showed saturated magnetization values of 16−17 μ_B. The nonsuperposition of the isofield curves is

(19) Yamamoto, S.; Matsuda, K.; Irie, M. *Angew. Chem., Int. Ed.* **2003**, *42*, 1636.

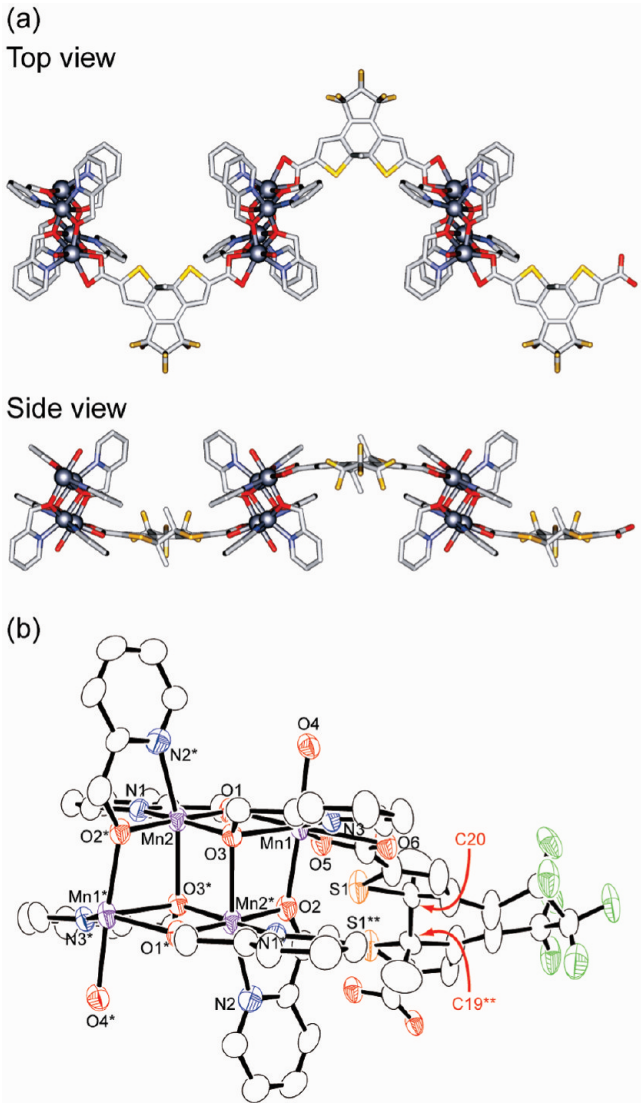

Figure 3. (a) 1-D chain structure and (b) ORTEP drawing of a repeating unit of **1c** (50% probability thermal ellipsoids). The disordered part in the dae-c^{2-} moiety and hydrogen atoms are omitted for clarity (see Figure S2). C(19)**−C(20) (indicated by red arrows) is the single bond in the closed-ring structure in the dae-c^{2-} moiety. Symmetry operation (*): $-x + 1, -y, -z + 1$; (**): $x, -y + {}^1/_2 - 1, -z$.

indicative of the presence of axial zero-field splitting, i.e., the axial zero-field splitting parameter (D) < 0.[15a,b] A best-fit simulation performed by using a matrix-diagonalization method taking into account only $S_T = 9$ and its axial zero-field splitting term (DS_{Tz}^2) afforded $g_{av} = 1.96$, $D/k_B = -0.31$ K for **1o** and $g_{av} = 1.88$, $D/k_B = -0.33$ K for **1c**. The obtained D value is similar to that of the previously reported [Mn_4] SMMs.[15,16b,d] In other words, both compounds have the potential to be SMMs. For SMMs with integer spins, the theoretical energy barrier for the magnetization relaxation, Δ, is expressed as $\Delta = |D|S_T^2$.[2] From the obtained D value and $S_T = 9$, the theoretical values Δ/k_B were estimated to be 25.1 and 26.7 K for **1o** and **1c**, respectively.

We are aware that the behavior of the magnetization even for **1c** (Figure 6) is close to that observed for isolated SMMs with negligible inter-SMM interaction or very weak interactions that only behave as a perturbation. Even at 1 T, the magnetization monotonically increased with a decrease in the temperature and hence followed the simulated curve. This indicates that the magnetic superexchange between [Mn_4] units with $S_T = 9$ through the dae bridge is very small, even in the closed-ring form (see the next section).

Single-Molecule Magnet Behavior in 1o and 1c. Ac magnetic susceptibility measurements were performed on microcrystalline samples with a 3 Oe oscillation field and a zero dc field as a function of the temperature and frequency (ν) to determine the SMM behavior of **1o** and **1c**. Figure 7 shows the temperature dependence of the ac susceptibilities (χ' is the real (in-phase) part and χ'' is the imaginary (out-of-phase) part) measured at several ac frequencies for **1o** and **1c**. As expected for SMMs, both χ' and χ'' were frequency-dependent, although a peak top of χ'', which indicates the freezing of the magnetization at a frequency, was not observed even at 1.8 K with 1500 Hz, suggesting slow relaxation of the magnetization of **1o** and **1c**. To estimate the relaxation time (τ) from the nonmaximum χ'' data, the χ'' vs ν data measured at fixed temperatures were simulated by using the Debye model for a distributed single-relaxation process of the magnetization (Figure 8).[20] From the simulated curve, τ can be determined at a specific temperature using the relation $\tau = 1/2\pi\nu_{max}$. The obtained relaxation times at several temperatures obeyed the Arrhenius law $\tau(T) = \tau_0 \exp(\Delta_{eff}/k_BT)$ (Figure 8) with $\Delta_{eff}/k_B = 9.2$ K, $\tau_0 = 3.2 \times 10^{-7}$ s and $\Delta_{eff}/k_B = 12.1$ K, $\tau_0 = 1.7 \times 10^{-7}$ s for **1o** and **1c**, respectively. Despite the rough estimation, the obtained τ_0 and Δ_{eff} values are comparable with those for previously reported [Mn_4] SMMs.[15,16b,d] Δ_{eff} was smaller than the theoretical value (Δ) estimated from $\Delta = |D|S_T^2$ using the D values obtained from the reduced magnetization measurements (vide supra). This is reasonable because the reversal of the magnetization of an SMM possibly involves not only the thermal activation over Δ but also the quantum tunneling of the magnetization (QTM), which is a "short-cut" through Δ. Thus, the smaller Δ_{eff} due to QTM in the ground state is typical even in the family of [Mn_4] SMMs. QTM should be suppressed by applying a dc field because of a mismatch between $+m_s$ and $-m_s$ magnetization levels by Zeeman splitting,[2b] which is evidence for SMM behavior. Ac measurements in the presence of an applied dc field afforded a larger Δ_{eff} value closer to Δ (Figure S3): $\Delta_{eff}/k_B = 12.8$ K with $\tau_0 = 9.9 \times 10^{-8}$ s for **1o** at 1 kOe and $\Delta_{eff}/k_B = 20.5$ K with $\tau_0 = 5.5 \times 10^{-9}$ s for **1c** at 2 kOe. The above ac magnetic data suggest that the each [Mn_4] unit in **1o** and **1c** behaves as an SMM.

The SMM behavior in **1o** and **1c** was also examined by measuring the field dependence of the magnetization (M vs H) at low temperatures. It should be mentioned that, as supposed from the ac data, no field hysteresis of the magnetization was observed at 1.8 K for both compounds (Figure S4). Further investigation was performed at 0.5 K on a field-oriented single crystal that was restrained in *n*-eicosane with an applied field of 70 kOe at 325 K, followed by cooling in the field (Figure 9). In the measurement, data were collected by applying fields at a scanning rate of 2 Oe s^{-1} parallel to the averaged easy axis direction of the [Mn_4] units in the crystals (see Experimental Section). **1o** showed a weak hysteretic response (butterfly−type hysteresis feature) with no coercive field (Figure 9a). On the other hand, **1c** showed a more distinct hysteresis loop with a small coercive field ($\approx$ 100 Oe) and several steps (Figure 9b). Some of these steps, for example at −1.3 and 1.1 kOe, can be

(20) (a) Cole, K. S.; Cole, R. H. *J. Chem. Phys.* **1941**, *9*, 341. (b) Aubin, S. M. J.; Sun, Z.; Pardi, L.; Krzystek, J.; Folting, K.; Brunel, L.-C.; Rheingold, A. L.; Christou, G.; Hendrickson, D. N. *Inorg. Chem.* **1999**, *38*, 5329.

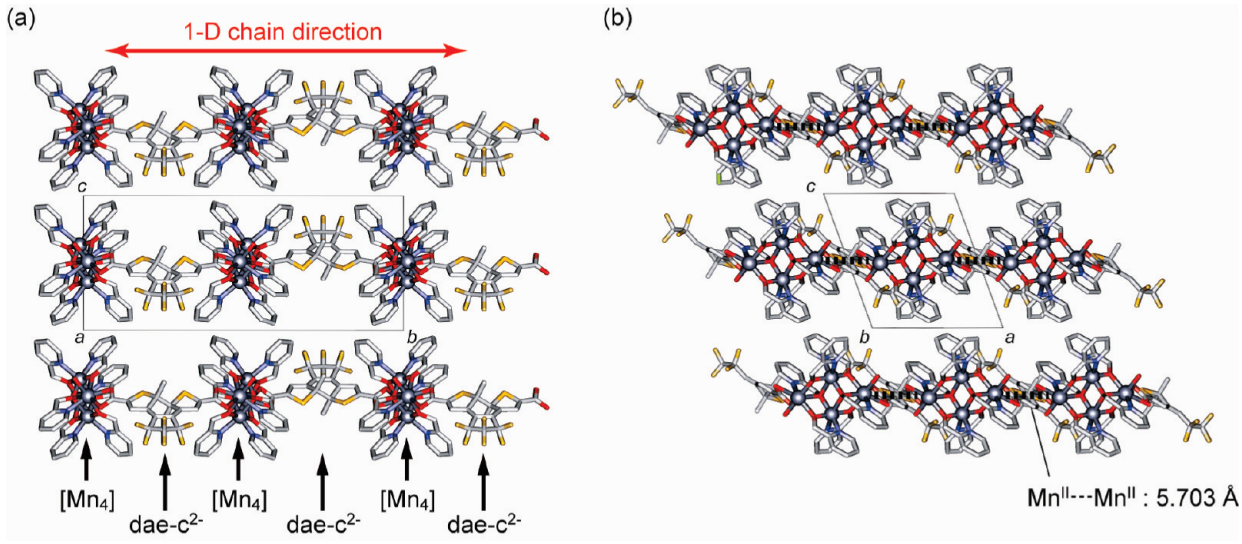

Figure 4. Packing diagrams of **1c** (a) projected along the *a* axis and (b) projected along the *b* axis, i.e., parallel to the chain axis. The hydrogen atoms, the acetonitrile and water molecules of crystallization, and ClO_4^- anions are omitted for clarity. The dotted lines in (b) denote the closest $Mn^{II}\cdots Mn^{II}$ contacts between the [Mn_4] cores in the neighboring chains.

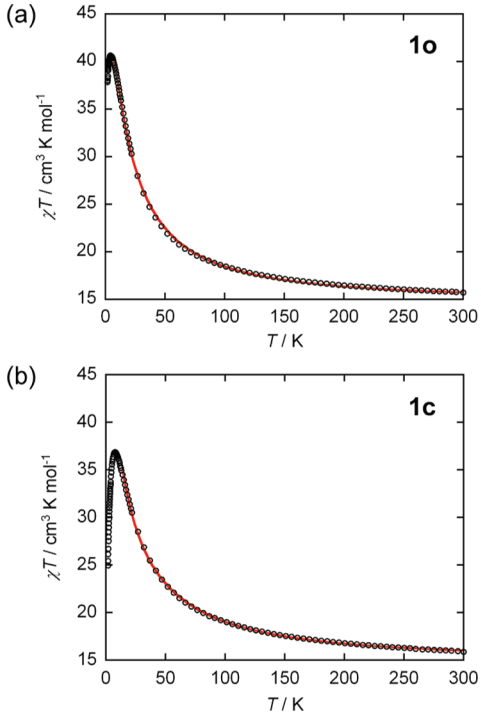

Figure 5. Temperature dependence of χT for (a) **1o** and (b) **1c** in a 1 kOe dc field. The red solid lines are the best-fitted simulation curves based on a tetranuclear Heisenberg model described in the text.

Table 2. Magnetic Parameters Obtained for **1o** and **1c**

	g	J_{wb}/k_B [K]	J_{bb}/k_B [K]	D/k_B [K]	Δ_{eff}/k_B [K]	
1o	1.96	1.26	9.18	−0.31	9.2 (zero dc field)	12.8 (1 kOe dc field)
1c	1.96	1.25	12.26	−0.33	12.1 (zero dc field)	20.5 (2 kOe dc field)

indicative of QTM, although the imperfect alignment of the crystal can cause a false step, such as that at $H = 0$. The step at ca. 3.5 kOe may be due to thermal activation. The steps at −1.3 and 1.1 kOe could be due to QTM between $m_s = 9$ and $m_s = -9$ and −8, respectively. From the field interval between the steps (ΔH = 2.4 kOe), a $|D|/k_B$ value of 0.32 K ($\Delta H \approx |D|/g\mu_B$) was determined,[4b,c,e] which agrees with the value

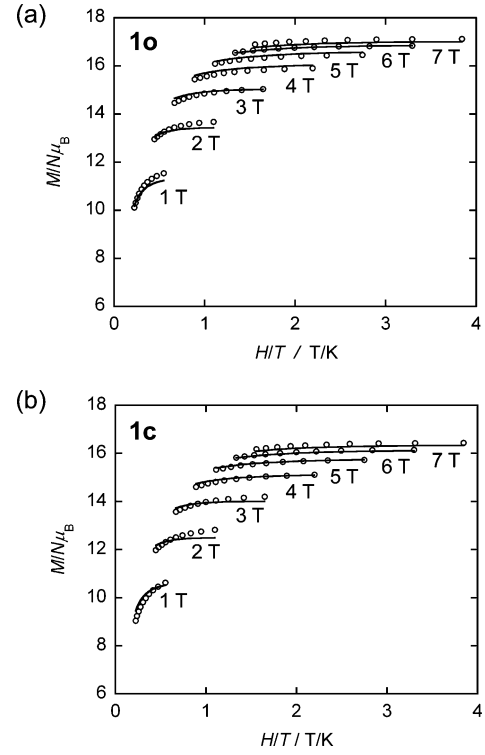

Figure 6. Plots of *M* vs *H*/*T* (1.8−4.5 K) for (a) **1o** and (b) **1c**. The solid lines are the best-fitted simulation curves obtained for $S_T = 9$ with $g_{av} = 1.96$, $D/k_B = -0.31$ K for **1o** and $g_{av} = 1.88$, $D/k_B = -0.33$ K for **1c**.

obtained from the reduced magnetization. It is noteworthy that the first step (−1.3 kOe) corresponding to QTM between $m_s = \pm 9$ was observed before the external field was decreased to zero. This shift in the field at which the QTM occurred suggests the presence of very weak antiferromagnetic interactions between the [Mn_4] units in **1c** ($|zJ|/k_B \approx 1 \times 10^{-2}$ K from $|zJ| = g\mu_B H_{ex}/2S_T$ with H_{ex} = 1.3 kOe = 0.13 T).[13] Albeit very small, these interactions could be the result of close inter-[Mn_4] contact between the neighboring 1-D chains (5.703 Å) and/or the inter-[Mn_4] connection through the dae-c^{2-} ligand in a chain.

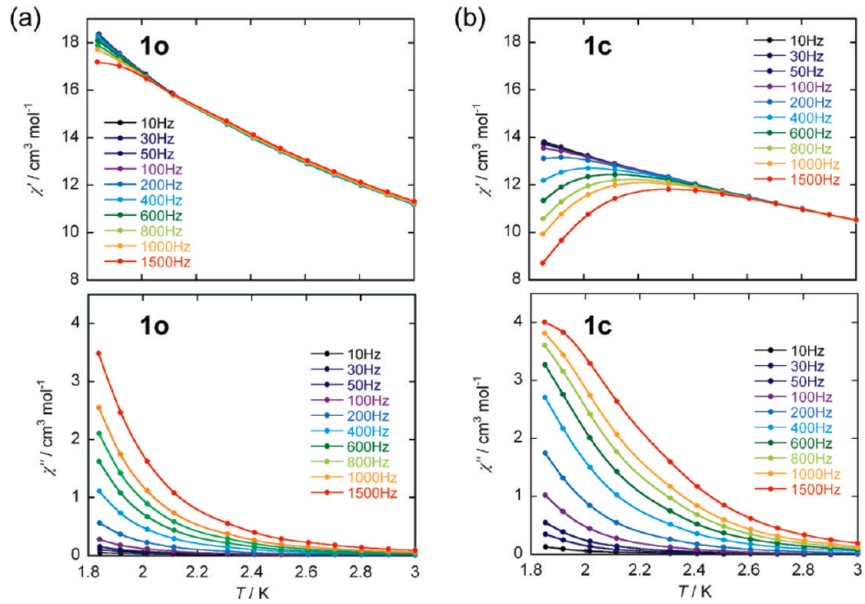

Figure 7. Temperature dependence of in-phase (χ') and out-of-phase (χ'') ac susceptibilities for (a) **1o** and (b) **1c** measured at several frequencies in a zero dc field and a 3 Oe oscillating ac field. The solid lines are guides.

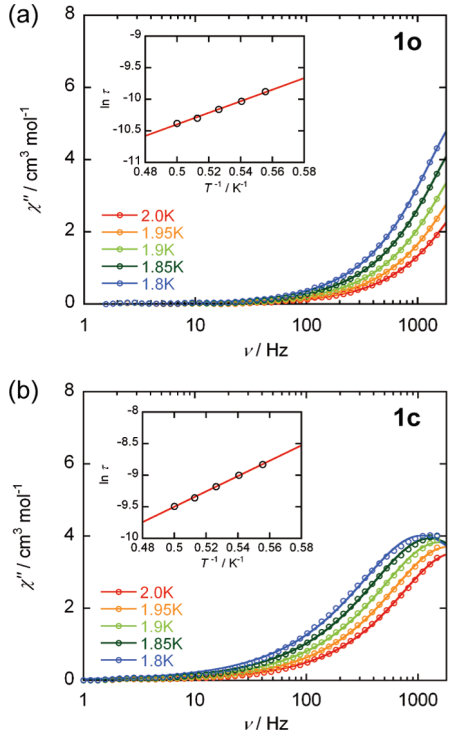

Figure 8. Ac-frequency dependence of χ'' measured at several temperatures in a zero dc field and 3 Oe oscillating ac field for (a) **1o** and (b) **1c**. The solid lines are the best-fitted simulation curves based on a generalized Debye model for the determination of the relaxation time. Insets are Arrhenius plots for relaxation times (τ) estimated from the simulations.

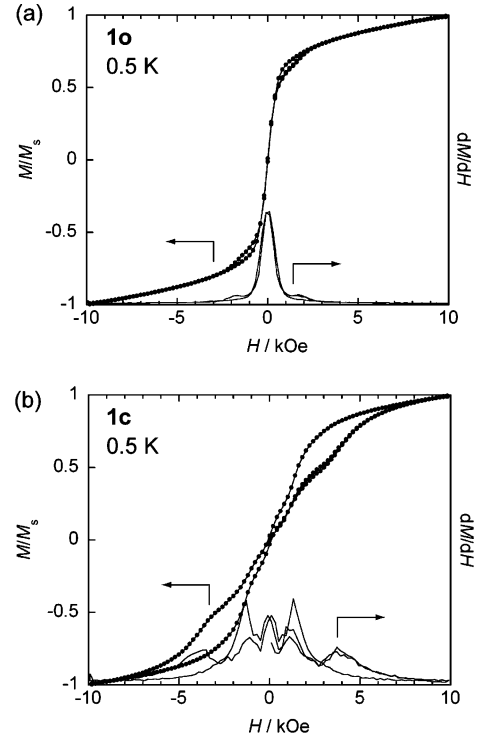

Figure 9. Plots of normalized M vs H and dM/dH vs H for field-oriented samples of (a) **1o** and (b) **1c** at 0.5 K.

Photochromic Reactions in 1o and 1c. It is well-known that the diarylethene group (dae) undergoes a reversible isomerization between open- and closed-ring isomers upon irradiation with UV (o → c) and visible light (c → o) even in the solid state, which causes a drastic color change characteristic of the chromophore of respective isomers.[11] The photochromic reactivity of **1o** and **1c** in the solid state was thus examined through visual color changes using KBr-diluted pellet samples of both compounds and changes in absorption spectra. Figure 10a shows photographs and absorption spectra of **1o**. Before photoirradiation, the **1o**-KBr pellet was reddish-brown due to the [Mn_4] chromophore (dae-o is colorless). Upon irradiation with UV light (λ = 313 nm), the **1o**-KBr pellet turned dark blue. This color change indicated that the dae-o moiety in **1o** underwent photocyclization to the corresponding closed-ring isomer (dae-c) in the crystal. Furthermore, irradiation of the blue pellet with visible light (λ > 480 nm) caused the initial reddish-brown one to return, indicating that the photogenerated closed-ring isomer also underwent cycloreversion to the open-ring isomer. In other words, the color change is photoreversible, and isomerization

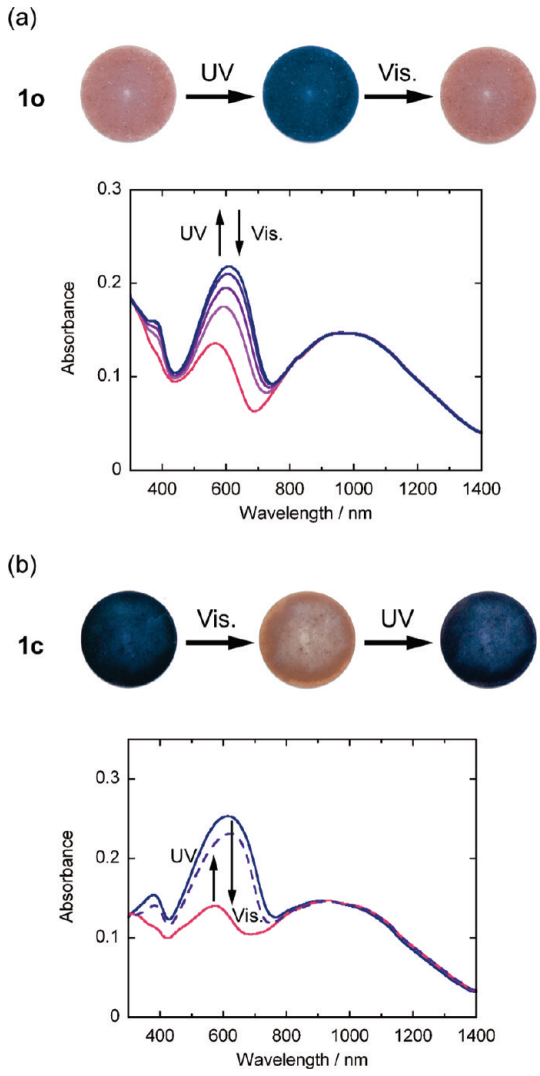

Figure 10. Photographs of KBr pellets, in which microcrystalline samples of (a) **1o** and (b) **1c** are dispersed, and absorption-spectral changes upon irradiation with UV (λ = 313 nm) and visible light (λ > 480 nm).

between the dae-o and dae-c isomers occurs reversibly in the solid state of **1o**. This reversible photochromic reaction was also examined by using absorption spectroscopy. Figure 10a also shows the photoinduced absorption-spectral changes of a powder sample of **1o** dispersed in a $BaSO_4$ matrix. Before photoirradiation, characteristic absorption bands around 580 and 980 nm corresponding to electronic transitions in the [Mn_4] chromophore were observed. Upon irradiation with UV light, a new absorption band appeared around 600 nm because of the formation of the dae-c isomer. This absorption band has been observed for the closed-ring isomer photogenerated in a single crystal of H_2dae-o.[9] As expected from the visual color change, the newly generated absorption band obtained by UV irradiation disappeared upon irradiation with visible light.

The photochromism of **1c** was also examined (Figure 10b). Before photoirradiation, the **1c**-KBr pellet was dark blue (consistent with the color of UV-irradiated **1o**). Upon irradiation with visible light, the pellet turned reddish-brown due to the photocycloreversion of the dae-c moiety to form dae-o. Then, upon irradiation with UV light, the pellet turned dark blue again, indicating that dae-c was regenerated by the photocyclization of the dae-o moiety. The changes in the absorption spectra shown in Figure 10b also corresponded to these photochromic

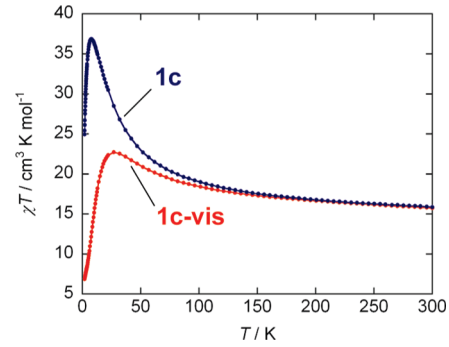

Figure 11. Temperature dependence of χT for **1c** and **1c-vis** in a 1 kOe dc field. The solid lines are guides.

reactions. The conversion ratio of the open- to closed-ring isomers in the photostationary state under photoirradiation at 313 nm was estimated to be 75% by comparing the absorbances at 600 nm for the closed-ring isomer before and after irradiation.

Effect of Photochromic Reactions on the Magnetic Properties. The effects of the photoinduced isomerization of dae on the magnetic properties was the main subject of this work. The dc and ac magnetic measurements were performed on a microcrystalline powder sample of **1o** irradiated at 313 nm for 26 h (denoted hereafter as **1o-UV**). The conversion ratio from the open- to closed-ring forms in **1o-UV** was estimated to be ~30% by measuring an absorption spectrum of the irradiated sample in a methanolic solution, and further irradiation did not increase the conversion. The relatively low conversion ratio is due to the inhomogeneity of the photoreaction, which mainly occurs near the surface of the crystalline powder, and/or the suppression of the conversion due to the simultaneous cycloreversion reaction. There was no significant change in X-ray powder diffraction (XRPD) patterns measured in the low 2θ angle range (5°−25°) between before and after the UV irradiation (Figure S5a). The magnetic data for **1o-UV** are shown in Figure S6. The data were the same as those for the unirradiated sample of **1o**, and no meaningful change in the magnetic properties was induced by photoirradiation.

In contrast, a drastic change in the magnetic properties of **1c** was observed after irradiation with visible light for 3 h. A microcrystalline powder sample of **1c** was irradiated until the conversion ratio was 100% determined from an absorption spectrum of a methanolic solution (hereafter denoted as **1c-vis**). XRPD data for **1c-vis** indicate that the crystallinity of the irradiated sample was preserved even after the 100% conversion (Figure S5b). The characteristic change between those of **1c** and **1c-vis** can be found as the somewhat shift of some diffraction peaks of **1c-vis** to lower angles, which suggests that the crystal structure underwent some modifications and the lattice was expanded by the geometrical change of the dae moiety accompanying its cycloreversion reaction. Simulations of their diffraction patterns allowed a rough estimatation of the cell parameters for **1c** and **1c-vis** and estimated a degree of change of cell parameters as $\Delta a = 1.83\%$, $\Delta b = -0.13\%$, $\Delta c = 3.69\%$, $\Delta\beta = -0.13\%$, and $\Delta V = 5.53\%$ using Δlattice(%) = (**1c-vis** − **1c**)/**1c** × 100. The *ac* plane, which includes the shortest [Mn_4]···[Mn_4] distance (5.703 Å along the *a* axis in **1c**), was in particular expanded despite no significant change in the *b* axis corresponding to the chain direction. Therefore, we suppose that this change is a key factor for the following magnetic change. Figure 11 shows the χT vs T data for **1c-vis** together with those of **1c**. Upon lowering the temperature, the

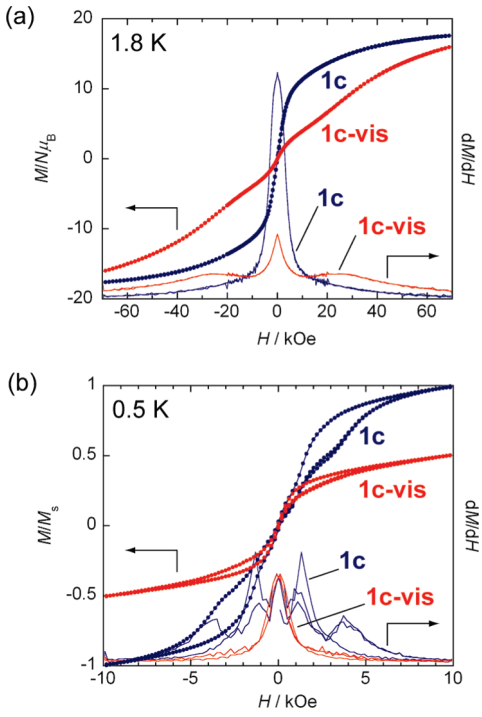

Figure 12. Plots of M vs H and dM/dH vs H for **1c** and **1c-vis** using (a) a nonorientation polycrystalline sample at 1.8 K and (b) field-oriented one at 0.5 K. M vs H data at 0.5 K were normalized with the saturated value for **1c** at 10 kOe.

χT value for **1c-vis** increased from 15.7 cm^3 K mol^{-1} at 300 K to 22.7 cm^3 K mol^{-1} at 27 K and then dropped sharply to 6.9 cm^3 K mol^{-1} at 1.8 K. The data for **1c** could be superimposed on those for **1c-vis** in the range 150−300 K. However, the data for **1c-vis** below 150 K were much smaller than those for **1c**, indicating that the photoinduced isomerization from dae-c to dae-o caused a change in the magnetic properties.

A large change induced by irradiation with visible light was also observed in the M vs H data. Figure 12a shows M vs H data at 1.8 K measured on random polycrystalline samples of **1c** and **1c-vis** restrained in Nujol. The magnetization of **1c-vis** showed a relatively rapid increase at low field strengths (2.5 μ_B at 5 kOe) and then increased quasi-linearly to 11.8 μ_B at ∼40 kOe with a broad inflection at ∼25.6 kOe, followed by a gradual increase to 16.0 μ_B at 70 kOe. The values at individual field strengths were considerably lower than those for **1c**. The M vs H data of **1c-vis** were also measured at 0.5 K using a field-oriented single-crystal sample (Figure 12b). A weak hysteresis response (butterfly−type) with no coercivity was observed for **1c-vis**. It should be noted that a similar inflection is also found in this measurement at almost the same field of $H_c \approx 26$ kOe (Figure S7). The inflection in the M vs H curve suggests the presence of intermolecular interactions among [Mn$_4$] units, in which antiferromagnetically coupled S_T spins of [Mn$_4$] units experience a flip when the magnitude of the interactions is overcome by an applied field H_c as seen in metamagnetic systems.[21] Similar behavior has been observed in antiferromagnetically ordered systems of a double-cuboidal [Mn$_4$] SMM[16d] and a square-shaped [Mn$_4$] SMM.[22] This

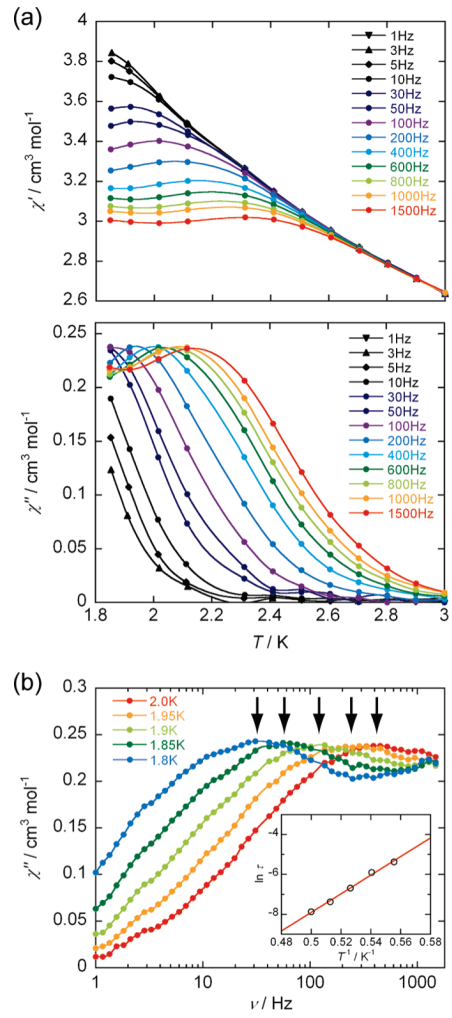

Figure 13. Plots of χ' and χ'' as a function of (a) temperature and (b) frequency for **1c-vis** in a zero dc field and a 3 Oe oscillating ac field. The arrows indicate peak tops due to the low-frequency relaxation mode. The solid lines are guides.

instability can be expressed as the Ising limit at 0 K: $H_c(0\ \mathrm{K}) = 2|zJ'|S_T/g\mu_B$, where z is the number of neighboring spins, J' is the antiferromagnetic coupling constant, and $S_T = 9$ for **1c-vis**.[23] Assuming $H_c(0) = 25.6$ kOe $= 2.56$ T, the magnetic interaction between the [Mn$_4$] units is estimated to be $|zJ'|/k_B \approx 0.19$ K. The dc data prove that the photoirradiation of visible light to **1c** indirectly enhances [Mn$_4$] interunit interactions. It is important to note that, considering the structural change upon isomerization from dae-c to dae-o induced by irradiation, the present [Mn$_4$] interunit interaction should be a through-space interaction (possibly in the *ac* directions) rather than a through-bond one via the dae-o linkage.

To gain further understanding of the magnetic properties of **1c-vis**, ac susceptibility measurements were performed (Figure 13). Similar to the χT vs T data in Figure 11, the values of χ' of **1c-vis** at low temperatures were smaller than the corresponding ones of **1c**; however, they were strongly frequency-dependent showing an increase in χ'' (Figure 13a). Furthermore, the maxima of χ'', which were not observed for **1c**, were observed above 1.8 K at ac frequencies in the range 200−1500 Hz. However, they were not single component values, indicating

(21) (a) Stryjewski, E.; Giordano, N. *Adv. Phys.* **1977**, *26*, 487. (b) Carlin, R. L. *Magnetochemistry*; Springer-Verlag: Berlin, 1986.
(22) Boskovic, C.; Bircher, R.; Tregenna-Piggott, P. L. W.; Güdel, H. U.; Paulsen, C.; Wernsdorfer, W.; Barra, A.-L.; Khatsko, E.; Neels, A.; Stoeckli-Evans, H. *J. Am. Chem. Soc.* **2003**, *125*, 14046.
(23) Chikazumi, S. *Physics of Ferromagnetism*; Clarendon Press (Oxford Science Publications): Oxford, 1997; p 521,

the existence of multiple relaxation processes. To determine the origins of the relaxation processes, ac susceptibilities were measured as a function of the ac frequency (1−1500 Hz) at several temperatures (Figure 13b). The χ'' vs ν data clearly showed the presence of two modes of relaxation: high-frequency and low-frequency modes. This has been observed for antiferromagnetically coupled [Mn$_4$] SMMs.[16d,22] Only in the low-frequency mode were peak tops observed in the frequency and temperature ranges measured (indicated as arrows in Figure 13b), and from an Arrhenius plot, $\tau_0 = 2.68 \times 10^{-14}$ s and $\Delta_{eff}/k_B = 46.7$ K. The value of τ_0 is much faster compared to general values observed for SMMs ($\tau_0 = 10^{-7}-10^{-10}$ s) and is similar to those of spin-glass-like materials that have short- and long-range multidomains.[24] In addition, the Δ_{eff}/k_B value is significantly larger than $\Delta/k_B = |D|S_T^2/k_B \approx 26$ K expected for **1o** and **1c**. Consequently, we attributed the slow relaxation to the effect of the [Mn$_4$] interunit antiferromagnetic short- and/or long-range ordering. The data in the high-frequency mode up to 1500 Hz at 1.8 K showing no peak tops were attributed to the relaxation of the magnetization of the [Mn$_4$] SMM unit. This hypothesis is supported by similar observations for other antiferromagnetically coupled [Mn$_4$] SMMs,[16d,22] where multiple relaxation processes are related to the applied ac frequencies. On the basis of dc and ac magnetic data, we concluded that the photocycloreversion of the dae-c moiety in **1c** caused the formation of a new magnetic phase, which combines the characteristics of [Mn$_4$] SMM unit and antiferromagnetic ordering.

Finally, to check the reversibility of this photoinduced change, the magnetic properties of **1c-vis** irradiated with UV light for 3.5 h (hereafter referred to as **1c-vis**−**UV**) were measured. The conversion ratio from the open to the closed form was 75%. After UV irradiation, the data nearly returned to those of **1c**; they were not identical because of the incomplete conversion of dae-o to dae-c and possible structural fluctuations (Figure S8). Nevertheless, in the case of the ac susceptibility data, the [Mn$_4$] interunit interactions observed in the low-frequency mode disappeared, and only the data for the high-frequency mode as well as those for **1c** remained (Figure 14). This reversibility indicates that the photoinduced change in the magnetic properties comes from the photoisomerization of the photochromic dae moiety.

Discussion of the Photoinduced Change in the Magnetic Properties. Here, we discuss the origin of the antiferromagnetic interactions in the visible-irradiated **1c-vis** and the difference in the photoresponsive behavior of **1o** and **1c**. As mentioned above, open-ring form **1o** exhibited no change in the magnetic properties after photocyclization with UV irradiation. On the other hand, closed-ring form **1c** underwent a significant photoinduced change in the dc and ac magnetic data: After the photocycloreversion with visible irradiation, we obtained credible magnetic data for **1c-vis** showing the presence of antiferromagnetic ordering of the S_T spins of the [Mn$_4$] units.

As mentioned in the introduction, we propose two plausible mechanisms to explain the photoswitching of the [Mn$_4$] interunit interactions: (I) direct switching of superexchange interactions through the π-system of the dae moiety (intrachain switching; Scheme 2a) and (II) indirect switching of the [Mn$_4$] interchain interactions due to the change in the distance between [Mn$_4$] units of neighboring 1-D chains (interchain switching; Scheme 2b). Mechanism I should occur preferentially with the closed-ring dae because the π-conjugation is spread over the entire molecule (Scheme 2a). However, the intermolecular magnetic interactions are greater in **1c-vis** having a dae-o moiety. Thus, mechanism I does not explain the occurrence of the antiferromagnetic interactions in **1c-vis**, whereas mechanism II does. The structural change in the dae moiety of **1c** from dae-c to dae-o upon photocycloreversion should cause a change in the packing geometry of [Mn$_4$] units or the arrangement of the 1-D chains (Scheme 3). The comparison of XRPD patterns between **1c** and **1c-vis** suggests that the structural change, in particular in the *ac* plane associated with interchain through-space interactions, was induced by the photoreaction (Figure S5). The short distance between relatively large spins with $S_T = 9$, as the *a* direction seen in **1c**, is more sensitive to changes in the structure, which strongly influences the [Mn$_4$] interunit interactions. Actually even in **1c**, there is a very weak antiferromagnetic interaction between the [Mn$_4$] units ($zJ/k_B \approx -1 \times 10^{-2}$ K). Since the dae derivatives change their geometrical structures, especially the position of their thiophene rings, during photocyclization and photocycloreversion in the single crystals,[11a,b] the crystal packing is greatly affected, sometimes leading to a large strain in the single crystal itself.[11f] The change may be small; however, it should be enough to trigger a significant enhancement of the antiferromagnetic interactions ($zJ/k_B \approx$

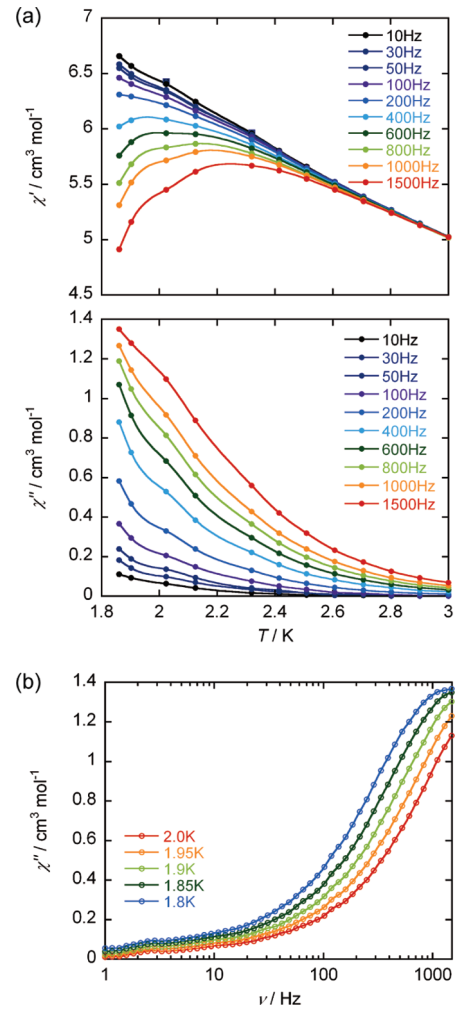

Figure 14. Plots of χ' and χ'' as a function of (a) temperature and (b) frequency for **1c-vis**−**UV** in a zero dc field and a 3 Oe oscillating ac field. The solid lines are guides.

(24) Mydosh, J. A. *Spin glasses: An Experimental Introduction*; Taylor and Francis: London, 1993.

Scheme 3. Proposed Mechanism for the Occurrence of the Antiferromagnetic Ordering in **1c-vis** after Irradiation with Visible Light, where the Arrows Indicate the Magnetization of SMM Aligned on an Easy Axis

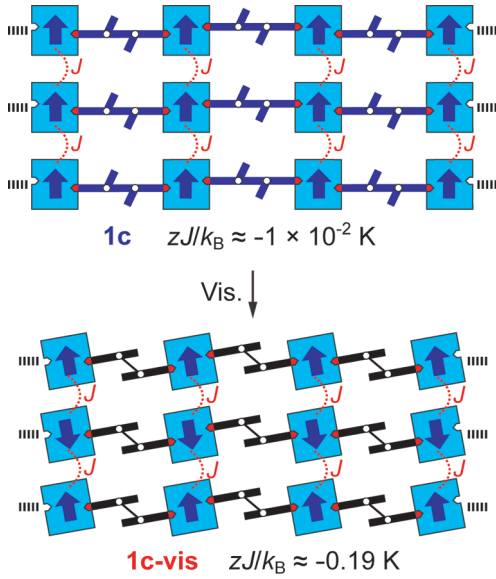

−0.19 K) because the distance between the [Mn_4] units in the initial **1c** is already fairly close.

The difference in the photoresponsive behavior of **1o** and **1c** is due to the difference in their packing structures. The closest Mn···Mn distance between the neighboring chains in **1o** is 8.453 Å, whereas, in **1c**, it is 5.703 Å. In other words, the structural change induced by photocyclization of the dae moiety in **1o** scarcely affected the [Mn_4] arrangement. In addition, the low conversion ratio from the UV-induced cyclization also hinders any drastic change in the magnetic properties.

Conclusion

In this paper, to the best of our knowledge, we prepared the first example of a coordination assembly of an SMM and a photochromic bridging ligand using a double-cuboidal [Mn_4] SMM and a diarylethene derivative with two carboxylate groups (dae). Using the open- and closed-ring forms of dae, dae-o^{2-} and dae-c^{2-}, afforded 1-D chain assemblies (**1o** and **1c**, respectively) with dae coordinating to the [Mn_4] via the carboxylate groups and with the SMM units and dae ligands in an alternating arrangement, [−{Mn_4}−(dae)−]. Dc and ac magnetic measurements on **1o** and **1c** showed that they behaved as SMMs with $S_T = 9$, similar to previously reported double-cuboidal [Mn_4] SMMs, despite being bridged by the dae groups. The open-ring form (dae-o) underwent photocyclization upon irradiation with UV to produce the closed-ring form (dae-c), and dae-c underwent photocycloreversion to dae-o upon irradiation with visible light. No significant change in the magnetic properties of **1o-UV** was observed when **1o** was photocyclized, although dae-c in **1o-UV** should have a well-conjugated π-pathway. In contrast, photocycloreversion for **1c** by visible irradiation (dae-c → dae-o) led to a drastic change in the magnetic behavior of **1c-vis**, and [Mn_4] interunit interactions were detected. The interactions were assigned to be through-space interactions rather than through-bond ones via the dae-o linkage, and they were caused by a change in the [Mn_4] arrangement between the neighboring 1-D chains due to the geometrical change in the dae moiety during the photoreaction. We concluded that the difference in the photoresponsive behaviors of **1o** and **1c** was due to the difference in the packing structures of the 1-D chains in the crystals.

The results obtained in this work illustrate the usefulness of the photochromic molecules for photoswitching of the magnetic behavior, even superparamagnetic behavior, in SMMs and will open the door to the development of an uncharted series of multifunctional and stimulus-responsive SMMs.[6] Photoswitching strongly depends on the packing structures of the crystals, and desirable functions are likely achieved by photoswitching of the through-bond magnetic pathways of a photochromic bridging ligand, as described in Scheme 2a. This work will enable the photoswitching of the spin dynamics (memory ON and OFF) of isolated photochromic SMM assemblies.

Experimental Section

General Procedures and Materials. All chemicals and solvents were used as received. The diarylethene ligands H_2dae-o and H_2dae-c were synthesized according to the same method as described in the literature.[9] All preparations and manipulations were carried out under aerobic conditions.

Synthesis of $[Mn_4(hmp)_6(dae\text{-}o)(ClO_4)_2]\cdot 6H_2O$ (1o). To an acetonitrile solution (20 mL) of manganese perchlorate hexahydrate (724 mg, 2.0 mmol) were added an acetonitrile solution (10 mL) of 2-hydroxymethylpyridine (546 mg, 5.0 mmol) and a 20 wt % aqueous solution of tetraethylammonium hydroxide (1.47 g, 2.0 mmol). After the mixture stirred for 15 min at room temperature, an acetonitrile solution (10 mL) of H_2dae-o (228 mg, 0.5 mmol) was added, and then the reaction solution was stirred for 1 h. The resulting solution was filtered and carefully layered on chloroform (80 mL) in a narrow diameter glass tube. After several days, black crystals of **1o** were obtained. Yield: 110 mg, 13% (based on Mn). Selected IR (KBr): 3429 (m), 2848 (m), 1606 (s), 1558 (s), 1481 (s), 1439 (s), 1404 (s), 1385 (s), 1371 (s), 1275 (s), 1186 (m), 1119 (s), 1045 (s), 984 (m), 810 (m) cm^{-1}. Anal. Calcd for $C_{53}H_{56}Cl_2F_6Mn_4N_6O_{24}S_2$: C, 39.06; H, 3.46; N, 5.16. Found: C, 39.19; H, 3.18; N, 5.16.

Synthesis of $[Mn_4(hmp)_6(dae\text{-}c)(H_2O)_2](ClO_4)_2\cdot CH_3CN\cdot 4H_2O$ (1c). The synthesis was carried out in a dark room to avoid the photocycloreversion reaction of the closed-ring isomer. To an acetonitrile solution (14 mL) of manganese perchlorate hexahydrate (489 mg, 1.4 mmol) were added an acetonitrile solution (7 mL) of 2-hydroxymethylpyridine (369 mg, 3.4 mmol) and a 20 wt % aqueous solution of tetraethylammonium hydroxide (994 mg, 1.4 mmol). After the mixture stirred for 15 min at room temperature, an acetonitrile solution (7 mL) of H_2dae-c (154 mg, 0.34 mmol) was added, and then the mixture was stirred for 1 h. The resulting solution was filtered and carefully layered on *m*-xylene (70 mL) in a narrow diameter glass tube. After several days, black needle crystals of **1c** were obtained. Yield: 84 mg, 14% (based on Mn). Selected IR (KBr): 3398 (m), 2843 (m), 1606 (s), 1579 (s), 1533 (m), 1483 (m), 1442 (s), 1387 (s), 1282 (m), 1228 (m), 1093 (s), 1043 (s), 1018 (s), 964 (s), 764 (s) cm^{-1}. Anal. Calcd for $C_{55}H_{59}N_7O_{24}Cl_2F_6Mn_4S_2$: C, 39.54; H, 3.56; N, 5.87. Found: C, 39.76; H, 3.63; N, 5.74.

Physical Measurements. Infrared spectra were measured as KBr pellets on a JASCO FT/IR-620 Fourier transform infrared spectrometer. Solid-state absorption spectra were measured in $BaSO_4$ matrices with a Shimadzu UV-3150 spectrophotometer. Photoirradiation was carried out with an Asahi Spectra MAX-301 300 W xenon lamp system. The wavelength was selected by passing the light through a band-pass filter or a cutoff filter. Magnetic measurements were obtained with the use of a Quantum Design MPMS-XL superconducting quantum interference device (SQUID) magnetometer. Dc measurements were collected in the temperature range 1.8−300 K and field amplitude range −70−70 kOe. Ac measurements were collected at various frequencies from 1 to 1488 Hz with an ac field amplitude of 3 Oe. Freshly prepared crystalline samples of **1o** and **1c** were used for the magnetic measurements to

avoid deterioration of the samples, and the measurements were performed using finely ground microcrystalline powder samples restrained in Nujol. Magnetization measurements at 0.5 K were obtained in an i-Quantum ^{3}He refrigeration system (i-Helium3)[25] attached to the MPMS-XL magnetometer. The measurements were performed on single-crystalline samples restrained in *n*-eicosane after prefield orientation by applying a field with an amplitude of 70 kOe at 325 K. The experimental data were corrected for the sample holder, the resin, and the diamagnetic contribution calculated from Pascal constants.[26]

Single-Crystal X-ray Analysis. Single crystals of **1o** and **1c** for X-ray crystallography were prepared by using the methods described in the synthetic procedure and mounted on a glass rod. Data collections were made on a Rigaku CCD diffractometer (Saturn 70) with graphite monochromated Mo Kα radiation (λ = 0.710 70 Å). The structures were solved by using direct methods (SIR 97)[27] and expanded using Fourier techniques.[28] The final cycles of full-matrix least-squares refinements on F^2 were converged with unweighted and weighted agreement factors of $R_1 = \Sigma||F_o| - |F_c||/\Sigma|F_o|$ ($I > 2.00\sigma(I)$ for R1 and all reflections for R), and $wR_2 = [\Sigma w(F_c^2 - F_c^2)^2/\Sigma w(F_c^2)^2]^{1/2}$ (all reflections). Neutral atom scattering factors were taken from Cromer and Waber.[29] Anomalous dispersion effects were included in F_{calcd}[30]; $\Delta f'$ and $\Delta f''$ were taken from Creagh and McAuley.[31] The mass attenuation coefficients were taken from Creagh and Hubbell.[32] All calculations were performed using the CrystalStructure[33,34] crystallographic software package. Crystallographic data for **1o** and **1c** are summarized in Table 1. CCDC-729109 for **1o** and CCDC-729108 for **1c** contain the supplementary crystallographic data for this paper. These data can be obtained free of charge from The Cambridge Crystallographic Data Centre via www.ccdc.cam.ac.uk/data_request/cif.

X-ray Powder Diffraction (XRPD). XRPD of **1o**, **1c**, **1o-UV**, and **1c-vis** were measured on a Rigaku RINT-2500HK diffractometer with Cu Kα radiation (λ = 1.5418 Å) at room temperature in the range $5° \le 2\theta \le 25°$, for which a well-grounded polycrystalline sample was put into a narrow diameter quartz glass tube.

Acknowledgment. We thank Prof. Takayoshi Kuroda-Sowa (Kinki University, Osaka, Japan) for simulations of the reduced magnetization and Prof. Brian Breedlove (Tohoku University, Sendai, Japan) for his helpful discussions. This work was supported by the CREST project of the Japan Science and Technology Agency (H.M. and M.Y.), a Grant-in-Aid for Scientific Research on Priority Areas (No. 17036054 "Chemistry of Coordnation Space") from the Ministry of Education, Culture, Sports, Science, and Technology, Japan (H.M.), and an Exploratory Research Program for Young Scientists of Tohoku University (M.M.).

Supporting Information Available: X-ray crystallographic files (CIF) for **1o** and **1c**; structural and magnetic data for **1o**, **1c**, **1o-UV**, **1c-vis**, and **1c-vis**−**UV** (Table S1, Figures S1−S8). These materials are free of charge via the Internet at http://pubs.acs.org.

JA903366D

(25) Shirakawa, N.; Horinouchi, H.; Yoshida, Y. *J. Magn. Magn. Mater.* **2004**, *272*−*276*, e149.
(26) Boudreaux, E. A., Mulay, L. N., Eds. *Theory and Application of Molecular Paramagnetism*; John Wiley & Sons: New York, 1976.
(27) Altomare, A.; Burla, M.; Camalli, M.; Cascarano, G.; Giacovazzo, C.; Guagliardi, A.; Moliterni, A.; Polidori, G.; Spagna, R. *J. Appl. Crystallogr.* **1999**, *32*, 115.
(28) Beurskens, P. T.; Admiraal, G.; Beurskens, G.; Bosman, W. P.; de Gelder, R.; Israel, R., Smits, J. M. M. *The DIRDIF-99 program system, Technical Report of the Crystallography Laboratory*; University of Nijmegen: The Netherlands, 1999.
(29) Cromer, D. T.; Waber, J. T. *International Tables for X-ray Crystallography*; The Kynoch Press: Birmingham, U.K., 1974; Vol. IV, Table 2.2A.
(30) Ibers, J. A.; Hamilton, W. C. *Acta Crystallogr.* **1964**, *17*, 781.
(31) Creagh, D. C.; McAuley, W. J. In *International Tables for Crystallography*; Wilson, A. J. C., Ed.; Kluwer Academic Publishers: Boston, 1992; Vol. C, Table 4.2.6.8, pp 219−222.
(32) Creagh, D. C.; Hubbell, J. H. In *International Tables for Crystallography*; Wilson, A. J. C., Ed.; Kluwer Academic Publishers: Boston, 1992; Vol. C, Table 4.2.4.3, pp 200−206.
(33) *CrystalStructure 3.8: Crystal Structure Analysis Package*; Rigaku and Rigaku Americas: 9009 New Trails Dr. The Woodlands, TX 77381, U.S.A., 2000−2007.
(34) Carruthers, J. R.; Rollett, J. S.; Betteridge, P. W.; Kinna, D.; Pearce, L.; Larsen, A.; Gabe, E. *CRYSTALS Issue 11*; Chemical Crystallography Laboratory: Oxford, U.K., 1999.